**Proceedings of the**
**International Conference on Mechanical Engineering and Renewable Energy 2017**
**(ICMERE2017) 18 – 20 December, 2017, Chittagong, Bangladesh**

**ICMERE2017-PI-134**

# FRACTURE MECHANICS BASED ANALYSIS OF FATIGUE CRACK RELATED ACOUSTIC WAVES

**Md Yeasin Bhuiyan**[1] **and Victor Giurgiutiu**[2]

[1,2]Department of Mechanical Engineering, University of South Carolina, Columbia 29208, USA
[1]Department of Mechanical Engineering, Bangladesh University of Engineering and Technology, Dhaka-1000, Bangladesh

Corresponding author: [1,*]yeasin85@gmail.com, [2]victorg@sc.edu

***Abstract***- *This paper presents the acoustic wave based method to capture the fracture mechanism of the fatigue crack. The fatigue experiments were performed to generate the fatigue crack with simultaneous measurement of the acoustic wave signals. The acoustic waves emit from the crack formation in the structure. The microscopic analysis of the fatigue crack was performed and showed that the crack advanced following a zigzag path. The crack path may follow the boundary of the weakest grain structures. These microscopic variations in the fatigue crack generate varieties of acoustic waves. The variation of the acoustic wave parameters may explain the complex fatigue crack formation in the structure. The crack initiation happened followed by a plastic deformation as the fatigue loading cycles continued. The crack nucleation triggers the acoustic wave generation. Certain parameter of acoustic wave signals is highly related to certain fracture parameters. The acoustic measurement provided a large amplitude, and a large number of AE hits before the final fracture. Thus the acoustic emission could be a damage precursor of the engineering structures.*

**Keywords:** Fracture mechanics, acoustic emission (AE). AE waveform, fatigue crack, crack nucleation

## 1. INTRODUCTION

Acoustic waves may occur in an engineering structure when the structural material undergoes sudden internal irreversible stress redistribution in its internal structure, for example, as a result of crack formation or plastic deformation [1], [2]. The stress waves are produced from these internal structural changes and result in acoustic emissions. Although the AE may contain a very wide range of frequencies but, most of the energy content of the acoustic waves is often in the ultrasonic regime (30 kHz – 1MHz). The acoustic emission (AE) based ultrasonic method has been widely used in multidisciplinary fields of engineering such as mechanical engineering, aerospace engineering, civil engineering, biomedical engineering [3]. This has been used for varieties of applications including flaw or leakage detection in pressure vessels, tanks, and piping systems. A significant use of the ultrasonic AE method is in the structural health monitoring (SHM) and nondestructive evaluation (NDE) field. They are using this method as a tool for in-situ structural damage evaluation and prognosis. The AE has also been used to monitor the corrosion and welding progress in engineering structures [4], [5].

There are many NDE techniques in a competition with the AE method such as visual, eddy current, liquid penetrate, magnetic particle, radiographic (x-ray and gamma ray), and thermo-graphic inspection. However, the AE method is advantageous since it needs relatively smaller sensors and they can be permanently bonded to the structure. This results in using the AE method as an SHM technique for continuous in-service monitoring of the structures while the other NDE techniques usually provide off-service monitoring.

The acoustic emission is considered to be a passive type SHM technique and requires less number of sensors as compared to an active SHM technique, another branch of the SHM [6]–[9]. The disadvantage of the AE method is that the conventional commercial AE systems can only estimate qualitative damage information of the structure. Nonetheless, they could localize the source of the damage using multiple sensors and triangulation algorithm. The current AE practice mostly rely on statistics based methods for the AE signal interpretation. The very few researchers including the current authors focused on the physics of material based methods for the AE signal interpretation.

The various parameters of an AE waveform were calculated that included average frequency, maximum amplitude, time of flight, duration, counts, and hits (Fig. 1) [10]. However, the examination of few AE waves provided very limited useful information of the AE from a crack growth. In fact, the complex nature of the AE wave generation, propagation, interaction with the

structural features made it much difficult to analyze individual AE waveforms. Most of the researchers focused on statistics based method in spite of physics of materials based approach.

In this paper, an acoustic wave method has been used to capture the fatigue fracture mechanism. The microscopic analysis was performed to interpretation the acoustic wave signals. The criticality of the structure was captured by the acoustic emission hit analysis that was related to the critical stress concentration factor (a fracture parameter). In addition, an AE waveform based method is outlined for extracting information of the crack propagation mechanism.

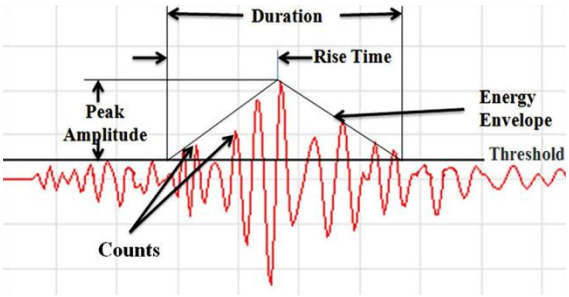


**Fig. 1**: A typical AE signals with varieties of parameters: peak amplitude, counts, duration, rise time, energy envelope, threshold [10]

## 2. BACKGROUND OF THE METHOD

The fracture mechanics based concepts can be employed to understand the physical meaning of the acoustic stress wave generated under mechanical load. The concepts of linear fracture mechanics is discussed in brief in this section. A comprehensive discussion on this is available in ref. [11]. Analysis of the fatigue damage in a given structure and predict the fatigue crack size is very important to maintain the structural integrity. There exist a critical crack size for which the crack will propagate spontaneously to failure under the specified loading. Maybe not all crack sizes are equally important to detect as the critical crack size. The crack size is related to the stress intensity factor as defined in Eq. (1).

$$K(\sigma,a) = C\sigma\sqrt{\pi a} \qquad (1)$$

where $\sigma$ is the applied stress, $a$ is the crack length, and $C$ is a constant depending on the specimen geometry and loading distribution. The critical crack size can be determined by Eq.(1) from the critical stress intensity factor It is remarkable that the stress intensity factor increases not only with the applied stress, $\sigma$, but also with the crack length, $a$. As the crack grows, the stress intensity factor also grows. If the crack grows too much, a critical state is achieved when the crack growth becomes rapid and uncontrollable. The value of $K$ associated with rapid crack extension is called the critical stress intensity factor, $K_c$. The critical stress intensity factor, $K_c$ can occur either for large value of stress with smaller crack size or for large crack length with smaller stress. For a given material, the onset of rapid crack extension always occurs at the same stress intensity value, $K_c$. For different specimens, having different initial crack lengths and geometries, the stress level, $\sigma$, at which rapid crack extension occurs, may be different. However, the $K_c$ value will always be the same. Therefore, $K_c$ is a property of the material. Thus, the condition for fracture to occur is that the local stress intensity factor $K(\sigma,a)$ exceeds the value $K_c$, i.e.,

$$K(\sigma,a) \geq K_c \qquad (2)$$

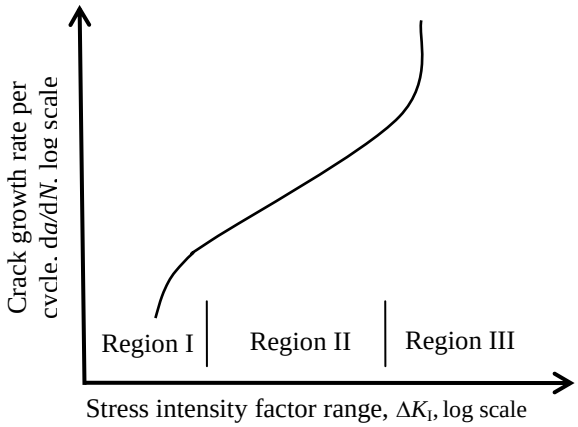


**Fig. 2**: Schematic representation of fatigue crack growth in metallic structures [11]

Experiments of crack length growth with number of cycles for various cyclic–load values have indicated that a high value of the cyclic load induces a much more rapid crack growth than a lower value [12]. It has been found that crack growth phenomenon has several distinct regions as depicted in Fig. 2. It shows three distinct regions:

I. Crack nucleation: an initial region in which the crack growth is very slow
II. Steady–state regime of linear crack growth in log-log coordinates. A linear region in which the log of the crack growth rate is proportional to the log of the number of cycles
III. Transition to the unstable regime: a nonlinear region in which the crack growth is very fast and rapidly leads to failure

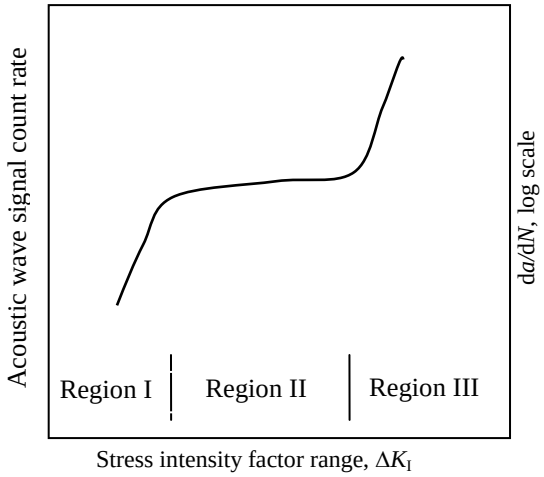


**Fig. 3**: Schematic representation of acoustic wave signal count rate variation with fatigue crack growth.

These three distinct regions have distinctive crack growth phenomena that may result in distinctive AE sources. The elastic waves generated from these AE sources may have specific characteristics. The typical AE signal has varieties of parameters such as peak amplitude, counts, duration, rise time, energy envelope, threshold (Fig. 1). Based on the AE source behavior, certain parameter may be affected more than the others. The count of an AE signals refers to the number of pulses emitted by the measurement circuitry if the signal amplitude is greater than the threshold. The schematic representation of the AE wave signal count rate is illustrated in Fig. 3. It shows three distinct region of the AE hit count rate:

I. An increasing trend in the acoustic wave signal count rate
II. A blunted linear region of almost constant acoustic count rate in the linear crack growth rate region
III. A steeper change in the count rate in the region where

Depending on the magnitude of the AE event and the characteristics of the material, one hit may produce one or many counts. While this is a relatively simple parameter to collect, it usually needs to be combined with amplitude and/or duration measurements to provide quality information about the shape of a signal. Several experiments showed that the count rate of AE signals variation with stress intensity factor [13].

In analyzing the fatigue crack growth, a famous article in ref. [14] determined that the fatigue crack–growth rate depends on the alternating stress and crack length.

$$\frac{da}{dN} = f(\Delta\sigma, a, C) \qquad (3)$$

where $\Delta\sigma$ is the peak–to–peak range of the cyclic stress, $a$ is the crack length, and $C$ is a parameter that depends on mean load, material properties, and other secondary variables.

Paris law is widely used in engineering practice. Further studies have revealed several factors that also need to be considered when applying Paris law to engineering problems. However, the Paris law is applicable to only linear portion of curve (Fig. 2).

The fatigue crack source processes such as microscopic crack jumps and precipitate fractures which may result in the acoustic wave signals. These processes are usually completed in a fraction of a microsecond or a few microseconds [15], [16]. Thus, the pulse due to AE source is usually short in duration [17], [18]. The amplitude and energy of the primitive pulse vary over an enormous range from submicroscopic dislocation movements to gross crack jumps. The acoustic waves from the fatigue crack source propagate in all directions. There often observed a directional dependency based on the nature of the fatigue crack mechanism. The complex fatigue crack growth mechanism may be explained by the nature of the acoustic wave signals.

The acoustic emission waveform contains all the individual parameters as discussed above as well as the frequency content. The frequency contents of the AE signals were found to be highly related to the AE source. Various signatures of the AE waveforms has been analyzed by the current authors before [19]. The AE sensor has also effect on the AE signals [20]. Multiphysics simulation has been performed to understand the fatigue crack behavior [21], [22]. The critical acoustic wave signals have been reported in this current paper. The AE hit evolution with the critical stress intensity factor has been discussed here.

## 3. EXPERIMENTAL SETUP

An in-situ AE-fatigue experiment was designed to apply the cyclic fatigue loading with simultaneous measurement of AE signals emanated from the fatigue crack growth. The wide specimen was manufactured for the fatigue test. It allowed a considerable amount of crack growth before failure. Aircraft grade aluminum Al-2024 T3 was used to make the. The dimension of the wide specimen was 100-mm (4 inches) in width, 305-mm (12 inches) in length and 1-mm in thickness. The experimental setup and an acoustic emission sensor bonded to the specimen was shown in Fig. 4. Three identical test coupons were made and tested under same loading conditions to for the repeatability of the experiment. A 1-mm diameter hole was drilled at the center of each test coupon. This facilitated stress concentration around the hole and eventually butterfly shaped crack was initiated. A hydraulic mechanical testing machine was used to apply cyclic fatigue loading to the specimen.

(a)

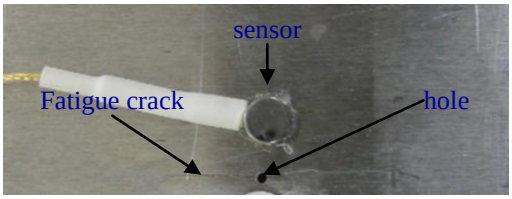


(b)

**Fig. 4**: (a) Experimental setup of the fatigue test with simultaneous measurement of acoustic emission, (b) An acoustic emission sensor bonded to the specimen. A fatigue crack is growing from the hole. (for scale: hole has 1-mm diameter)

The cyclic loading was applied in two stages. At first stage of loading, the cyclic loading was varied from

11.5 kN (maximum) to 1.15 kN (minimum) with the frequency of 1 Hz and R ratio ( R ratio = $F_{min} / F_{max}$ ) of 0.1. At the second stage, the cyclic loading was reduced to 90% of the first stage loading maintaining the same R ratio. The cyclic loading frequency was reduced to 0.2 Hz. At the second stage, the fatigue crack was grown at controlled manner avoiding sudden failure. This also facilitated in-situ AE measurement with fatigue crack growth.

## 4. RESULTS AND DISCUSSION

The experimental results were acquired from many different aspects. Three simultaneous systems were running: (i) fatigue loading using the MTS, (ii) optical measurement of fracture path, (iii) acoustic emission measurement. The fatigue loading is not discussed here for the sake of brevity. The microscopic data analysis and the acoustic emission results are discussed next.

### 4.1 Microscopic Analysis of Fatigue Cracks

A very high magnification digital microscope has been used to observe the crack formation path. During the fatigue test, a continuous video recording of the crack growth was performed using a high-resolution digital Basler camera. This allowed optical measurement of the crack growth with fatigue cycle. However, this was not sufficient to pinpoint the crack tip and extract the exact crack length. For this reason, the high magnification (2000-5000X) microscope was also employed for the fracture path visualization. It was observed that no significant change was observed optically until 28,000 fatigue cycles. The fatigue test specimen was examined intermittently under the high magnification microscope during the entire test.

It was observed that butterfly shaped plastic deformation occurred around the hole as illustrated in Fig. 5a. The specimen was further loaded to the fatigue loading machine and the fatigue cycle was continued. The overall substantial change in the fatigue crack was monitored using the in-situ camera whereas the diminutive change was examined under the microscope. It was found that the butterfly shaped plastically deformed path eventually turned into a fracture path. During this plastic deformation, the crack nucleation occurred inside the material. Since the nucleation happened sub-surface it was not observed during the microscopic observation on the surface of the material.

The plastic deformation was noticed on the both side of the hole that looked like a dent from the naked eye. Both plastic deformations were about the same length that was marked by the two red ellipses. However, the inclination of the plastic crack nucleation was different. The left side plastic deformation was horizontal while the right side plastic deformation was little inclined to the horizontal line (Fig. 5a). This may be because of the manufacturing imperfection of maintaining homogeneity in the material, and the shape of the grain boundaries of the material. The micro structural grain boundaries of the aluminum material may affect the path of the crack growth.

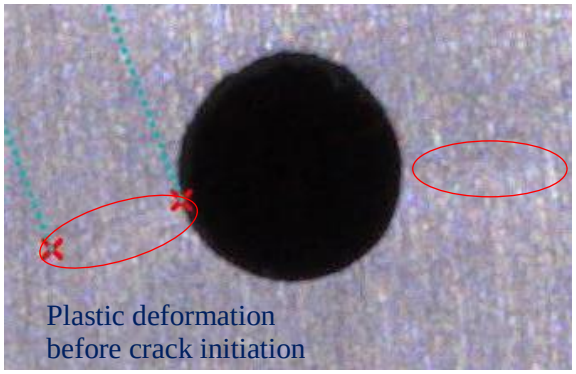


(a) Plastic deformation around the hole

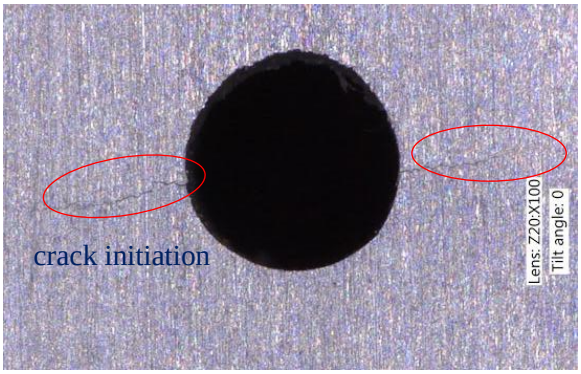


(b) Crack initiation followed by plastic deformation

**Fig. 5**: Microscopic observation of the crack formation. A digital microscope has been used for the exact crack length measurement. The plastic deformation occurred under cyclic fatigue loading that was eventually converted into a crack initiation.

After the crack nucleation, the crack started to grow as the fatigue cycle continued. The initiated crack is illustrated in Fig. 5b. It can be noted that the crack path is not straight. The zigzag nature of the crack path had been clearly observed from the exaggerated view as shown in Fig. 5b. The fatigue loading was continued after the examination under the microscope. Several microscopic measurements were performed but not all of them are shown here for brevity. The microscopic analysis revealed that the crack growth happened following a zigzag path rather than a straight line.

### 4.2 Acoustic Emission (AE) Measurement during Fatigue Crack Growth

The acoustic emission (AE) was measured by using specialized equipment (from Mistras Inc.) for this purpose. The in-situ measurement was performed. The acoustic wave signals were captured by a commercial AE sensor while the fatigue crack grew. A preamplifier (40 dB) recommended by the same manufacturer was used with AE instrumentation. There was no significant AE signal emanated from the specimen until the crack nucleation occurred. During the initial crack formation, some AE signals were captured. However, the signal to noise ratio was relatively low. When the cracks started to grow at an average rate of 1.32 μm/cycle and a greater number of AE signals were generated from the fatigue cracks. The count rate of the AE signals was found to be

larger than the previous AE signals as illustrated in Fig. 3. The evolution of the AE hits gives the indication of the microscopically observed crack growth phenomena.

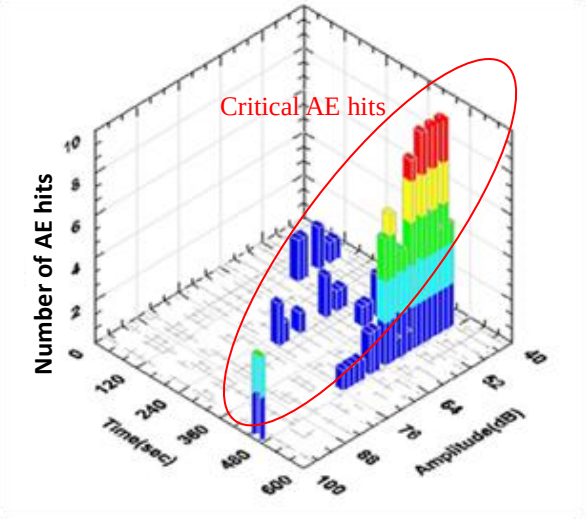


**Fig. 6**: The 3-D plot of the critical acoustic emission hits before fracture. The number of AE hits increased drastically when the spontaneous crack propagation occurred. The critical AE hits gave the indication of the critical stress concentration before the final fracture of the specimen.

The AE signals were captured by setting a threshold limit. The threshold was set to a relatively lower value (40 dB) that was equal to the preamplifier gain. The threshold was selected when the AE system was not picking up environmental noise anymore. When the amplitude of any AE signal crossed the threshold, it was recorded as an AE hit. Numerous AE hits were captured during the fatigue crack growth. Each AE hit had a corresponding AE waveform.

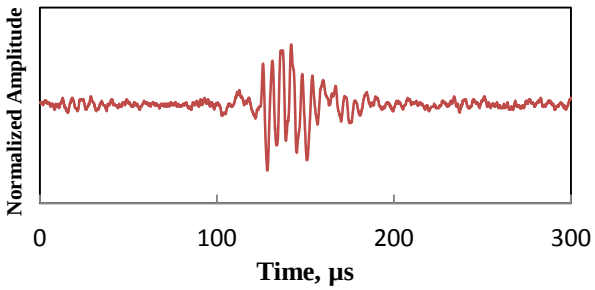


**Fig. 7**: A typical AE signal captured during fatigue crack growth. A time duration of 300-µs was chosen for the data acquisition. The main acoustic wave packet lied within 120-µs -180-µs.

At the very end of the fatigue cycles, the crack grew very fast and the specimen was prone to fracture. To understand the behavior of the AE hit and amplitude just before fracture, the cyclic loading rate was decreased and some critical AE hits were captured. The 3-D plot is shown in Fig. 6. and it shows that the number of AE hits increased significantly before the final fracture. It is also noticed that the maximum amplitude jumped from 52 dB to 98 dB before the fracture. Since a large number of material grain structures broke when the crack grew longer, the material released a larger amount of energy in the form of acoustic emission. These emissions corresponded to a large number of AE hits and higher amplitudes of the AE signals. This transition of the AE hit signified the critical stress concentration factor after which spontaneous crack growth occurred and lead to final fracture of the structures.

Within the AE hit, there are much more information buried in the AE waveform. Hence, the AE waveform analysis was also performed. The most common AE waveform observed from the experimental results is shown in Fig. 7. The length of the AE signal is sufficiently long to accommodate the complete waveform. Thus, it could be observed that there were calm periods before and after the main time domain AE signal (120-180 µs). The long time domain signal ensured all AE features to be captured in an AE waveform.

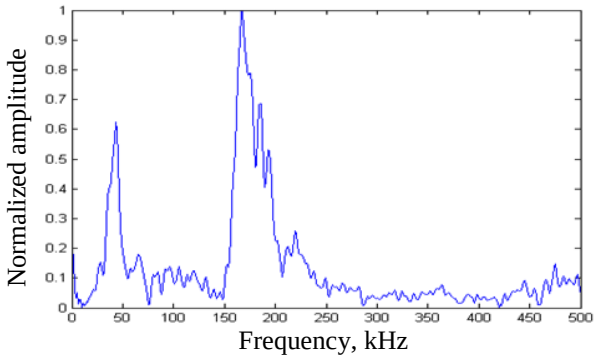


**Fig. 8**: The frequency spectrum of the acoustic wave signals. The fast Fourier transform (FFT) has been performed to the time-domain signal to obtain the frequency spectrum. Two main frequency peaks can be observed around 50-kHz and 160-kHz.

Fast Fourier transform (FFT) provided the frequency spectrum of the AE signal as shown in Fig. 8. Higher sampling rate allowed better resolution of the frequency spectrum. Two main peaks could be observed: one near 50 kHz and another near 160 kHz. These frequency peaks are related to the fatigue crack growth. Some frequency peaks also happen around 190 kHz, 195 kHz, and 220 kHz. These frequency peaks may be associated with the zigzag nature of the fatigue cracks. However, the AE signal interaction with the crack may generate some frequency peaks that need further investigation.

## 5. CONCLUSION

In this paper, the fracture mechanics based analysis of the fatigue crack was performed by using acoustic emission (AE) method. The acoustic waves occured during the fatigue crack evolution in the structure. The AE waveforms could provide the signature of fatigue crack growth. The microscopic analysis of the fatigue crack was performed and showed that the crack advanced following a zigzag path. The crack path may follow the boundary of the weakest grain structures. The crack initiation occurs following a plastic deformation path. The crack nucleation triggers the acoustic wave generation. Certain parameters of acoustic wave signals are highly sensitive to certain fracture parameters. The

acoustic measurement provided a large amplitude, and a large number of AE hits before the final fracture. Thus the acoustic emission could be a damage precursor of the engineering structures.

## 6. FUTURE WORK

This is an ongoing research and has many potential applications in the industries. Further investigator of this method would be performed in near future. The waveform based analysis of the acoustic emission that was introduced in this paper may provide very useful for capturing the fatigue crack growth mechanism.

## 7. ACKNOWLEDGEMENT

Support of Office of Naval Research, the U.S. Navy, Grant#N00014-14-1-0655, Dr. Ignacio Perez Program Manager, is thankfully acknowledged.

## 8. REFERENCES

[1] R. K. Miller, E. K. Hill, and P. O. Moore, *Nondestructive Testing Handbook: Acoustic Emission Testing*, 3rd ed. Columbus, OH, USA: American Society for Nondestructive Testing, 2005.

[2] T. Kishi, M. Ohtsu, and S. Yuyama, *Acoustic Emission - Beyond the Millennium*. Elsevier, 2000.

[3] K. Grabowski, M. Gawronski, I. Baran, W. Spychalski, W. J. Staszewski, T. Uhl, T. Kundu, and P. Packo, "Time–distance domain transformation for Acoustic Emission source localization in thin metallic plates," *Ultrasonics*, vol. 68, pp. 142–149, 2016.

[4] C. K. Lee, P. D. Wilcox, B. W. Drinkwater, J. J. Scholey, M. R. Wisnom, and M. I. Friswell, "Acoustic Emission during Fatigue Crack Growth in Aluminium Plates," *Proc. ECNDT*, vol. Mo.2.1.5, pp. 1–8, 2006.

[5] T. M. Roberts and M. Talebzadeh, "Acoustic emission monitoring of fatigue crack propagation," *J. Constr. Steel Res.*, vol. 59, no. 6, pp. 695–712, 2003.

[6] M. Y. Bhuiyan, Y. Shen, and V. Giurgiutiu, "Guided Wave Based Crack Detection in the Rivet Hole Using Global Analytical with Local FEM Approach," *Materials (Basel).*, vol. 9, no. 7, p. 602, 2016.

[7] M. Y. Bhuiyan, Y. Shen, and V. Giurgiutiu, "Interaction of Lamb waves with rivet hole cracks from multiple directions," *Proc. Inst. Mech. Eng. Part C J. Mech. Eng. Sci.*, vol. Online, no. January, 2017.

[8] M. Y. Bhuiyan, "Guided wave inspection of cracks in the rivet hole of an aerospace lap joint using analytical-FEM approach," University of South Carolina, 2016.

[9] M. Y. Bhuiyan, Y. Shen, and V. Giurgiutiu, "Ultrasonic inspection of multiple-rivet-hole lap joint cracks using global analysis with local finite element approach," in *Health Monitoring of Structural and Biological Systems 2016*, 2016, vol. 9805, pp. 1–15.

[10] S. Agcaoglu and O. Akkus, "Acoustic Emission Based Monitoring of the Microdamage Evolution During Fatigue of Human Cortical Bone," *J. Biomech. Eng.*, vol. 135, no. 8, pp. 1–8, 2013.

[11] V. Giurgiutiu, *Structural health monitoring with piezoelectric wafer active sensors*, 2nd ed. Elsevier Academic Press, 2014.

[12] J. A. Collins, *Failure of Materials in Mechanical Design*. John Wiley & Sons, 1993.

[13] M. Huang, L. Jiang, P. K. Lia, C. R. Brooks, R. Seeley, and D. L. Klarstrom, "Using Acoustic Emission in Fatigue and Fracture Materials Research," *J. Miner. Met. Mater. Soc.*, vol. 50, no. 11, 1998.

[14] P. Paris and F. Erdogan, "A Critical Analysis of Crack Propagation Laws," *J. Fluids Eng.*, vol. 85, no. 4, pp. 528–534, 1963.

[15] M. Y. Bhuiyan, J. Bao, B. Poddar, and V. Giurgiutiu, "Toward identifying crack-length-related resonances in acoustic emission waveforms for structural health monitoring applications," *Struct. Heal. Monit. Int. J.*, vol. Online, pp. 1–9, 2017.

[16] M. Y. Bhuiyan, J. Bao, B. Poddar, and V. Giurgiutiu, "Analysis of acoustic emission waveforms from fatigue cracks," in *Proceedings of SPIE (Health Monitoring of Structural and Biological Systems)*, 2017, vol. 10170, p. 101702A–1–8.

[17] M. G. R. Sause and S. Richler, "Finite element modelling of cracks as acoustic emission sources," *J. Nondestruct. Eval.*, vol. 34, no. 1, pp. 4, 2015.

[18] W. H. Prosser, M. A. Hamstad, J. Gary, and A. O'Gallagher, "Finite Element and Plate Theory Modeling of Acoustic Emission Waveforms," *J. Nondestruct. Eval.*, vol. 18, no. 3, pp. 83–90, 1999.

[19] M. Y. Bhuiyan and V. Giurgiutiu, "The Signatures of Acoustic Emission Waveforms from Fatigue Crack Advancing in Thin Metallic Plates," *Smart Materials and Structures*, no. Accepted, p. SMS-105887, 2017.

[20] M. Y. Bhuiyan, B. Lin, and V. Giurgiutiu, "Acoustic emission sensor effect and waveform evolution during fatigue crack growth in thin metallic plate," *J. Intell. Mater. Syst. Struct.*, vol. online, pp. 1-10, 2017.

[21] R. Joseph, M. Y. Bhuiyan, and V. Giurgiutiu, "Acoustic emission source modeling in a plate using buried moment tensors," in *Proceedings of SPIE (Health Monitoring of Structural and Biological Systems)*, 2017, pp. 1017028-1–8.

[22] M. Y. Bhuiyan and V. Giurgiutiu, "Multiphysics simulation of low-amplitude acoustic wave detection by piezoelectric wafer active sensors validated by in-situ AE-fatigue experiment," *Materials (Basel)*, Vol. 10, No. 8, pp.1-18, 2017.

## 9. NOMENCLATURE

| Symbol | Meaning | Unit |
|---|---|---|
| $\sigma$ | Stress | (Pa) |
| $K$ | Stress intensity factor | ( $Pa\sqrt{m}$ ) |
| $a$ | Crack length | (m) |
| $N$ | Number of cycle | (dimensionless) |